MOLECULAR AND CELLULAR BIOLOGY, Jan. 2000, p. 372–378 Vol. 20, No. 1
0270-7306/00/$04.00+0


# *INK4d*-Deficient Mice Are Fertile Despite Testicular Atrophy

FREDERIQUE ZINDY,[1] JAN VAN DEURSEN,[2] GERARD GROSVELD,[2] CHARLES J. SHERR,[1,3] AND MARTINE F. ROUSSEL[1]*

*Departments of Tumor Cell Biology[1] and Genetics[2] and Howard Hughes Medical Institute,[3] St. Jude Children's Research Hospital, Memphis, Tennessee 38105*

Received 26 August 1999/Returned for modification 21 September 1999/Accepted 22 September 1999

**The INK4 family of cyclin-dependent kinase (CDK) inhibitors includes four 15- to 19-kDa polypeptides ($p16^{INK4a}$, $p15^{INK4b}$, $p18^{INK4c}$, and $p19^{INK4d}$) that bind to CDK4 and CDK6. By disrupting cyclin D-dependent holoenzymes, INK4 proteins prevent phosphorylation of the retinoblastoma protein and block entry into the DNA-synthetic phase of the cell division cycle. The founding family member, $p16^{INK4a}$, is a potent tumor suppressor in humans, whereas involvement, if any, of other INK4 proteins in tumor surveillance is less well documented. *INK4c* and *INK4d* are expressed during mouse embryogenesis in stereotypic tissue-specific patterns and are also detected, together with *INK4b*, in tissues of young mice. *INK4a* is expressed neither before birth nor at readily appreciable levels in young animals, but its increased expression later in life suggests that it plays some checkpoint function in response to cell stress, genotoxic damage, or aging per se. We used targeted gene disruption to generate mice lacking *INK4d*. These animals developed into adulthood, had a normal life span, and did not spontaneously develop tumors. Tumors did not arise at increased frequency in animals neonatally exposed to ionizing radiation or the carcinogen dimethylbenzanthrene. Mouse embryo fibroblasts, bone marrow-derived macrophages, and lymphoid T and B cells isolated from these animals proliferated normally and displayed typical lineage-specific differentiation markers. Males exhibited marked testicular atrophy associated with increased apoptosis of germ cells, although they remained fertile. The absence of tumors in *INK4d*-deficient animals demonstrates that, unlike *INK4a*, *INK4d* is not a tumor suppressor but is instead involved in spermatogenesis.**

Cell proliferation is positively regulated by cyclin-dependent kinases (CDKs), and in normal cells, progression through the $G_1$ phase of the cell cycle depends upon the activities of cyclin D-dependent CDK4 or CDK6, and later, on cyclin E- and A-dependent CDK2 (reviewed in reference 45). These holoenzymes cooperate to phosphorylate the retinoblastoma protein (Rb), canceling its growth-suppressive function and initiating an E2F-dependent transcriptional program that is necessary for entry into the DNA synthetic (S) phase of the cell cycle (reviewed in references 7 and 49). In addition, cyclin E-CDK2 complexes phosphorylate additional substrates whose modifications are required for $G_1$ exit and initiation of DNA replication (reviewed in reference 39).

The activities of the $G_1$ CDKs can be blocked by CDK inhibitors (CKIs) that, in mammalian cells, fall into one of two distinct families (reviewed in references 44 and 46). The INK4 class (Inhibitors of CDK4) consists of four members ($p16^{INK4a}$, $p15^{INK4b}$, $p18^{INK4c}$, and $p19^{INK4d}$) that exclusively bind to and inhibit the cyclin D-dependent catalytic subunits CDK4 and CDK6. By contrast, the Cip/Kip family includes three members ($p21^{CIP1}$, $p27^{KIP1}$, and $p57^{KIP2}$) that bind to both cyclins and CDKs to preferentially inhibit cyclin E- and A-dependent CDK2.

CKIs act cooperatively during the $G_1$ phase of the cell division cycle. As cells enter the cycle from quiescence and progress through $G_1$ phase, Cip/Kip proteins initially act as positive regulators of the cyclin D-dependent kinases, aiding in their mitogen-dependent assembly, stabilization, and nuclear import (5, 21) and remaining associated with cyclin D-CDK complexes without inhibiting their activities (2, 21, 47, 51). (In this context, the term CDK inhibitor is a misnomer.) Apart from assembling into active complexes with D-type cyclins and Cip/Kip subunits, CDK4 and CDK6 can alternatively enter into inactive binary complexes with INK4 proteins, which may normally serve as a sink for any unutilized or improperly folded CDK subunits. The balance between formation of these different CDK4- and CDK6-containing complexes is likely set by the accumulation of cyclin D regulatory subunits in response to mitogenic stimulation (driving assembly of active complexes containing Cip/Kip proteins) and, conversely, by certain antiproliferative signals that can act to increase the relative concentrations of INK4 proteins (reviewed in reference 44). Kinetic studies performed both in vitro and in vivo have indicated that the association of INK4 proteins with CDK4 prevents Cip/Kip binding, and vice versa (36), consistent with more recently obtained structural data (3, 41) (reviewed in reference 32). During $G_1$ phase progression, the sequestration into higher-order cyclin D-CDK complexes of Cip/Kip proteins lowers their effective inhibitory threshold, thereby enabling cyclin E- and A-dependent CDK2 to become active as cells approach the $G_1$-to-S-phase transition. On the other hand, by binding to CDK4 or CDK6, induced INK4 proteins disrupt cyclin D-dependent kinases, canceling their activities and liberating the latent pool of Cip/Kip proteins, which can then act to inhibit CDK2. Therefore, the enforced expression of INK4 proteins in mammalian cells inhibits the activity of all $G_1$-phase CDKs and induces growth arrest by preventing entry into the S phase of the cell cycle (1, 16, 23–25, 31, 36, 37).

Although they appear to be structurally redundant and equally potent as inhibitors, the INK4 family members are differentially expressed during mouse development (54). *INK4c* and *INK4d* are widely expressed during mouse embryogenesis while *INK4a* and *INK4b* expression are undetectable before birth. By 4 weeks of age, $p15^{INK4b}$, $p18^{INK4c}$, and

* Corresponding author. Mailing address: Department of Tumor Cell Biology, St. Jude Children's Research Hospital, 332 North Lauderdale, Memphis, TN 38105. Phone: (901) 495-3481. Fax: (901) 495-2381. E-mail: martine.roussel@stjude.org.

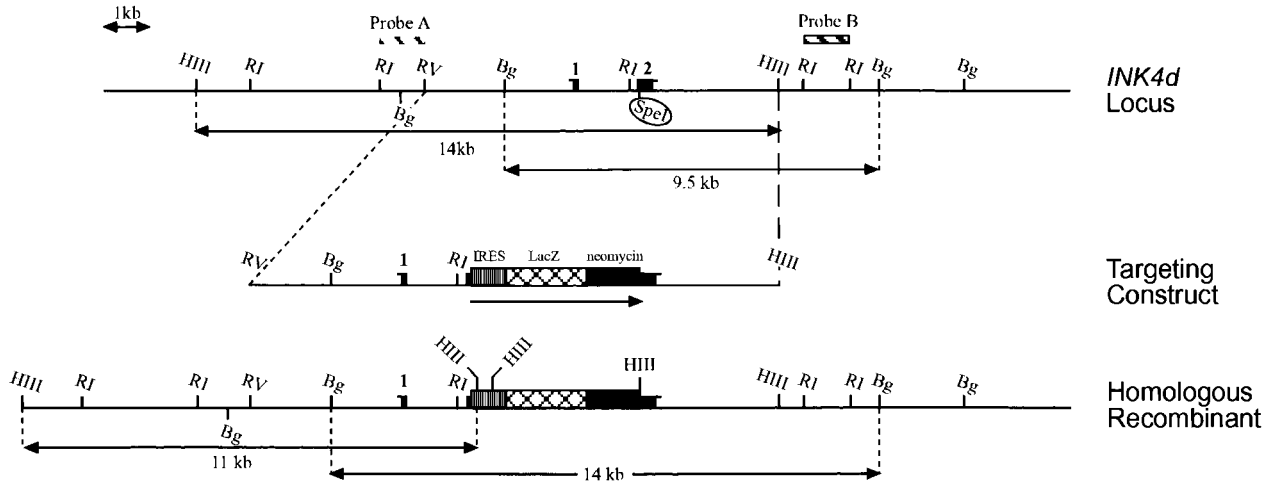


FIG. 1. Mouse INK4d locus, targeting vector, and targeted allele. The upper line shows a map of the *INK4d* locus with exons 1 and 2 defined by filled bars and various restriction sites indicated. R1, *Eco*RI; HIII, *Hin*dIII; Bg, *Bgl*II; RV, *Eco*RV. The unique *Spe*I site in exon 2 is circled. A β-*geo* gene flanked by an internal ribosome entry site (IRES) was inserted into the *Spe*I site in exon 2 to generate the targeting cassete. The map of the recombined locus is shown by the lower line. Probes A and B corresponding to restriction fragments flanking *INK4d* coding sequences (top) are predicted to differentially hybridize to the *Hin*dIII and *Bgl*II fragments defined at the top (wild-type allele) and at the bottom (mutant allele).

$p19^{INK4d}$ can be detected in many mouse tissues, but $p16^{INK4a}$ protein expression is initially restricted to the lung and spleen of somewhat older mice, with increasing and more widespread expression becoming manifest as the animals age. In humans, $p16^{INK4a}$, the founding member of the family (42), functions as a potent tumor suppressor, whereas the roles of other INK4 family members, if any, in tumorigenesis remain largely anecdotal (40). Mice deficient in *INK4a* develop normally and are highly cancer prone (43). However, these animals also lack the $p19^{ARF}$ product of the *INK4a* alternative reading frame (33), whose disruption (with retention and expression of $p16^{INK4a}$-coding sequences) reproduces the same tumor-prone phenotype (17). Hence, the formal demonstration that $p16^{INK4a}$ acts as a tumor suppressor in mice awaits the production of animals that lack *INK4a* but retain alternative reading frame function.

Mice deficient in *INK4c* develop gigantism and widespread organomegaly; middle lobe pituitary tumors later in life (9); and, less commonly, seminomas, adrenal pheochromocytoma, and renal glomerulopathies (M. Barbacid, personal communication). These animals display increased numbers of lymphoid B and T cells, with the cells undergoing accelerated proliferation upon mitogenic stimulation (9). Disruption of *INK4b* leads to extramedullary hematopoiesis and to formation of secondary follicles in lymph nodes as well as to tumors of various tissues in a small percentage of animals. When crossed onto an *INK4c*-null background, *INK4b* loss did not exacerbate the abnormalities observed in *INK4c*-deficient mice (M. Barbacid, personal communication). This may seem surprising in retrospect, given the fact that $p15^{INK4b}$ is strongly induced by transforming growth factor β (11, 37), while $p18^{INK4c}$ is induced by interleukin-6 (IL-6) (26).

Here, we show that deletion of *INK4d* in the mouse, like that of other *INK4* members, does not affect mouse development. *INK4d*-deficient mice showed no gross anomalies, had a normal life span, and did not develop tumors, and primary cells of different lineages isolated from these animals had unremarkable proliferative properties. Males displayed marked testicular atrophy associated with increased apoptosis, without apparently compromising their fertility.

## MATERIALS AND METHODS

**Targeting of *INK4d*.** The genomic DNA encoding the *INK4d* gene was cloned from a bacteriophage library prepared from 129/sv embryonic stem (ES) cells using a full-length murine *INK4d* cDNA probe (12). A 14-kb *Eco*RV-*Hin*dIII fragment containing the two coding exons was isolated. A cassette containing the *lacZ* gene (β-*geo*) fused to the neomycin resistance gene was inserted in the second coding exon at a unique *Spe*I site, and the targeting vector was electroporated into E14R3M4 ES cells. Correct homologous recombination occurred at 7.6% frequency as determined by Southern blotting analysis of ES cell DNA. DNA was digested with *Bgl*II or *Hin*dIII, was separated on an agarose gel, was transferred to nitrocellulose, and was hybridized with a 3′ (probe B) or a 5′ (probe A) probe (Fig. 1). Probe B detects a 9.5-kb fragment in the wild-type allele and a 14-kb fragment in the mutant allele. Probe A detects a 14-kb fragment from the wild-type allele and an 11-kb fragment in the DNA of mutant mice. Mice were routinely genotyped by isolating tail DNA and digesting it with *Bgl*II followed by Southern blotting analysis using probe B.

**Histology, in situ hybridization, protein analysis, and TUNEL assays.** Male mice were overdosed with intraperitoneal injections of ketamine and rompun and perfused intracardially with a fixative containing 4% paraformaldehyde in 0.1 M sodium phosphate buffer, pH 7.6, for 20 min. Isolated testes were postfixed in the same solution for 4 h at 4°C and were transferred into 25% sucrose in 0.1 M sodium phosphate buffer, pH 7.6, at 4°C for an additional 24 h. Sections of 12-μm thickness were cut with a cryostat, were mounted on Fisher brand Super-frost-plus slides, and were stored at −20°C. For routine histology, sections were stained with 0.05% toluidine blue in a solution containing Walpole's acetic acid and sodium acetate buffer, pH 4.4. In situ hybridization (55) and immunoblotting analysis (54) were performed as previously described. Terminal deoxynucleotidyltransferase-mediated dUTP-biotin nick end labeling (TUNEL) assays were performed by using the ApopTag detection kit (Oncor, Gaithersburg, Md.), essentially following manufacturer's instructions with minor modifications depending upon the specimen preparation. In brief, sections were postfixed for 15 min in 4% paraformaldehyde, were washed twice with phosphate-buffered saline (PBS), and were incubated in ethanol-acetic acid (2:1) for 5 min at −20°C. After two washes in PBS, sections were subjected to a proteinase K digestion (10 μg/ml in 10 mM Tris HCl, pH 8.0, and 1 mM EDTA), were washed twice with PBS, and were counterstained with methyl green. β-Galactosidase staining was performed as previously described (29). Tissues were counterstained with 1% neutral red in a solution containing Walpole's acetic acid and sodium acetate buffer.

## RESULTS

**Targeted disruption of *INK4d* in the mouse.** We disrupted the mouse *INK4d* gene by homologous recombination in ES cells (Fig. 1). The $p19^{INK4d}$ protein is a 166-amino-acid polypeptide encoded by two exons: exon 1 (codons 1 to 47) and exon 2 (codons 48 to 166) (12). We inserted a β-*geo* cassette containing *LacZ* fused to the neomycin resistance (*neo*) gene

into the second exon of *INK4d*. Seven independent ES cell clones, screened for homologous recombination by Southern blotting analysis, were microinjected into blastocysts from C57BL/6 mice to generate chimeric animals. Two chimeric mice, derived from two independently targeted ES cell clones, transmitted the disrupted allele through the germ line after breeding with C57BL/6 mice. The phenotypes of both independently derived mouse strains, as described below, are identical.

Heterozygotes were mated to produce founder strains of all three genotypes, including *INK4d* wild-type mice (+/+), heterozygotes (+/−), and nullizygotes (−/−), each verified by Southern blotting analysis of tail DNA (Fig. 2A). We detected no expression of $p19^{INK4d}$ protein in testes (Fig. 2B) or other organs (see below) of *INK4d*-deficient animals, while the levels of $p19^{INK4d}$ protein in tissues of heterozygous animals were approximately half those detected in their wild-type littermates (Fig. 2B). In situ mRNA hybridization and immunostaining confirmed the absence of *INK4d* mRNA expression and demonstrated expression of β-galactosidase in place of $p19^{INK4d}$ (see below). Furthermore, the loss of $p19^{INK4d}$ protein expression in various tissues from *INK4d*-deficient mice was not compensated by detectable increases in the expression of other INK4 proteins (Fig. 2C). As noted previously (54), $p15^{INK4b}$, $p18^{INK4c}$, and $p19^{INK4d}$ could be readily detected in different tissues of 2-month-old animals, whereas $p16^{INK4a}$ expression was conspicuously absent at this time. Pertinent to results that follow, $p15^{INK4b}$, $p18^{INK4c}$, and $p19^{INK4d}$ were each expressed in testes, although $p19^{INK4d}$ predominated.

**Viability and phenotypic analysis of *INK4d*-deficient mice.** Interbreeding of *INK4d* heterozygotes yielded offspring at a normal Mendelian ratio (25.5% +/+, 54.2% +/−, and 22.3% −/−; total of 238 mice) indicating that, in spite of the expression of *INK4d* during normal embryogenesis (54), its loss did not affect fetal development or survival. Apart from abnormalities in testicular size and male germ cell maturation (see below), no other overt developmental anomalies were observed in *INK4d*-deficient animals, which were fertile and had an otherwise uncomplicated and normal life span.

Given that human $p16^{INK4a}$ acts as a potent tumor suppressor (reviewed in reference 40) and that mice lacking $p18^{INK4c}$ develop middle lobe pituitary tumors (9) and, less often, seminomas and adrenal pheochromocytomas (M. Barbacid, personal communication), we explored the possibility that *INK4d* might play a role in tumor suppression. A cohort of 50 *INK4d*-deficient mice was observed for spontaneous tumor development for more than 2 years. Eight animals died of unknown causes in their second year of life at a frequency indistinguishable from that of their wild-type littermates (7 of 59), all without evidence of tumor pathology. Cohorts of *INK4d*-deficient mice treated neonatally with ionizing radiation or with the carcinogen dimethylbenzanthrene did not develop tumors at sites or rates that were significantly different from those seen in wild-type mice (27, 35). Together, these data failed to provide evidence that $p19^{INK4d}$ acts as a tumor suppressor.

Primary cells isolated from the *INK4d*-deficient animals, including mouse embryo fibroblasts (MEFs), bone marrow-derived macrophages and pro-B cells, thymic T cells, and splenic B cells, showed no cell cycle, proliferative, or differentiative anomalies (data not shown). For example, MEFs from *INK4d*-deficient embryos and their wild-type counterparts grew at the same rate, reached identical saturation densities, and entered senescence after a similar number of population doublings. Serum-starved *INK4d*-null MEFs exited the cell cycle normally and, when restimulated with mitogens, entered S phase at the same rate as their wild-type counterparts. The cells exhibited

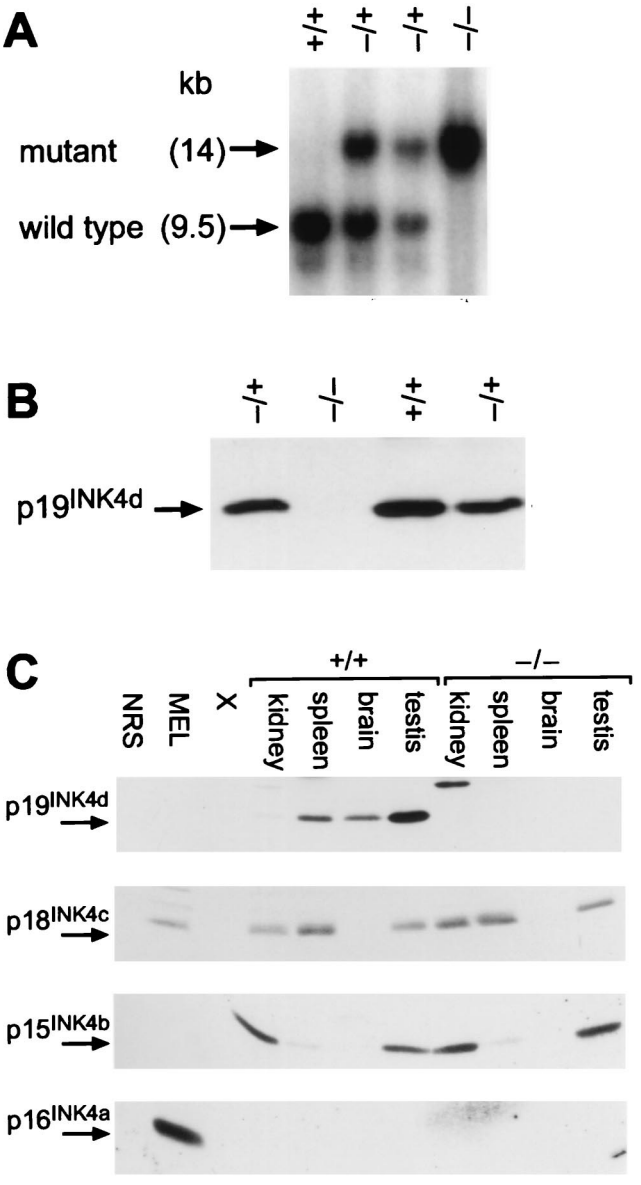


FIG. 2. *INK4d* genotype and expression. (A) Southern blotting analysis of tail DNA taken from littermates derived from interbred $INK4d^{+/-}$ hemizygotes. DNA was digested with *Bgl*II, was transferred to nitrocellulose, and was hybridized with probe B (Fig. 1, top). (B) $p19^{INK4d}$ protein expression in testes from mice of the indicated genotypes, as determined by sequential immunoprecipitation and immunoblotting. (C) INK4 protein expression in kidney, spleen, brain, and testis from 8-week-old wild-type (+/+) and *INK4d*-null (−/−) mice determined as for panel B. Mouse erythroleukemia (MEL) cells were used as a positive control for $p16^{INK4a}$ and $p18^{INK4c}$ expression.

anchorage-dependent growth and were not sensitive to transformation by oncogenic Ha-*Ras*. Although $p19^{INK4d}$ is highly expressed in spleen and thymus (54), T and B lymphocytes derived from both spleen and thymus of these animals exhibited normal responses to lymphokines, as measured by their proliferation rates in culture, and displayed cell surface markers characteristic of their lineage. Pre- and pro-B cells cultured on IL-7-producing feeder layers (50) also exhibited characteristic lineage-specific markers without perturbation of differentiation. Bone marrow-derived macrophages from *INK4d*-deficient animals displayed the expected dependence on colony-stimulating factor-1 for proliferation and survival.

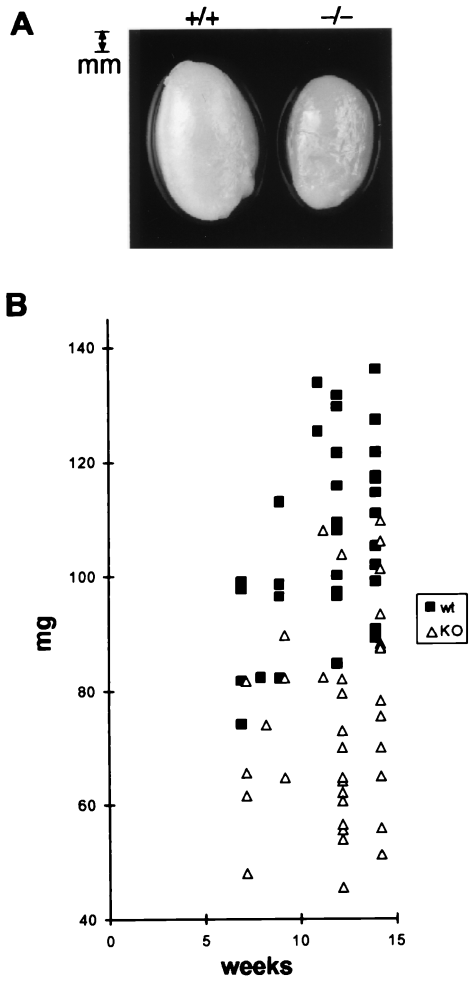


FIG. 3. Testicular atrophy in *INK4d*-deficient males. (A) Testes from 4-month-old wild-type (+/+) and *INK4d*-deficient (−/−) mice. (B) Comparison of the weights of wild-type (squares) and *INK4d*-deficient (triangles) testes at different ages of development. Additional data and statistical parameters are summarized in Table 1.

Moreover, although IL-10 treatment of mouse bone marrow-derived macrophages leads to growth arrest associated with induction of $p19^{INK4d}$, the macrophages explanted from the *INK4d*-deficient mice showed partial impairment in their ability to undergo arrest in response to IL-10 (30).

**Testicular atrophy and increased apoptosis in *INK4d*-null animals.** Visual examination at autopsy revealed obvious testicular atrophy in *INK4d*-deficient adult animals (Fig. 3A). Testes of males from all genotypes were weighed and measured between 7 and 14 weeks after mouse birth (Fig. 3B and Table 1). A statistically significant reduction in size (30 to 40%) was observed in the testes of *INK4d*-deficient animals ($P < 0.01$), whereas mice of all genotypes had comparable body weights. Histologic sections of testes from 3-month-old *INK4d*-deficient mice revealed that atrophy resulted from an overall reduction in size of the seminiferous tubules (Fig. 4C versus A and Fig. 4I versus H). Spermatozoa were nonetheless visualized in the lumina, consistent with the fact that fertility was not critically compromised in these animals.

To analyze *INK4d* expression in testes, we performed in situ hybridization of tissue sections from adult wild-type mice using an antisense *INK4d* cDNA probe (Fig. 4B). Germ cell development begins at the periphery of the tubule where spermatogonia reside. These cells give rise to the progressively more differentiated spermatocytes and spermatids that populate the more superficial tubular layers, and ultimately yield mature spermatozoa that can normally be visualized in the tubular lumina (reference 38 and references therein). *INK4d* RNA staining was visualized throughout the tubular diameter, consistent with the idea that the gene is expressed in differentiating germ cells. No signal above background was observed in sections from *INK4d*-deficient testes (Fig. 4D). Since *INK4d*-deficient mice were generated by inserting a *lacZ* gene into exon 2 of the gene, β-galactosidase expression under control of the *INK4d* promoter could reciprocally be observed in heterozygous and nullizygous mice by histochemical staining (Fig. 4F and G). As expected, staining of sections from *INK4d*-deficient testes revealed translumenal patterns of β-galactosidase expression in tissues of both $INK4d^{+/-}$ and $^{-/-}$ mice, with heavier and more widespread staining observed in testes of animals that lacked both copies of the gene (Fig. 4G versus F). In testis sections from *INK4d*-deficient mice, we also observed many giant cells which appeared to correspond to apoptotic bodies that were not seen frequently in sections from wild-type mice (Fig. 4I [arrows] versus H). Consistent with this interpretation, we detected a significant increase in TUNEL-positive cells in testis sections from *INK4d*-deficient animals (Fig. 4K versus J). Therefore, *INK4d* plays a role in male germ cell development, but its loss is insufficient to completely compromise sperm cell production.

## DISCUSSION

**Deletion of *INK4d* alone does not compromise mouse development or lead to tumor formation.** Among the four *INK4* family members, *INK4d* is the most ubiquitously expressed. Yet, despite *INK4d* RNA expression throughout embryonic development and in virtually all mouse tissues examined (54), its targeted disruption did not affect fetal or adult development, and animals lacking $p19^{INK4d}$ function enjoyed a normal and otherwise uncomplicated life span. Moreover, despite the fact that neonatally irradiated and dimethylbenzanthrene-treated C57BL/6 mice develop lymphomas and skin tumors (17, 27, 35, 43), respectively, treated *INK4d*-deficient mice developed neither a greater number of tumors nor more aggressive tumors than wild-type littermates exposed to the same insults.

TABLE 1. Testicular weight versus body weight in wild-type and *INK4d*-deficient mice[a]

| Mouse age and genotype (no. analyzed)[b] | Mean wt (SD) (g) | Minimum wt (g) | Maximum wt (g) |
|---|---|---|---|
| 12 weeks old | | | |
| Testis WT (11) | 0.108 (0.015) | 0.084 | 0.131 |
| Testis KO (13) | 0.067 (0.015) | 0.045 | 0.104 |
| Body WT (9) | 25.9 (2.77) | 21.8 | 30.1 |
| Body KO (10) | 28.3 (2.07) | 24.8 | 31.0 |
| 14 weeks old | | | |
| Testis WT (13) | 0.111 (0.013) | 0.089 | 0.136 |
| Testis KO (13) | 0.082.2 (0.018) | 0.051 | 0.110 |
| Body WT (13) | 29.4 (2.90) | 25.2 | 34.1 |
| Body KO (13) | 27.1 (2.36) | 24.1 | 30.5 |

[a] Differences in testis weight were statistically significant between these two groups of animals ($P < 0.01$). Body weight, however, was not significantly different between wild-type and *INK4d*-deficient mice.

[b] Statistical analysis was performed by comparing testis weight and body weight from two groups of wild-type (WT) or *INK4d*-deficient (KO) animals of either 12 or 14 weeks of age.

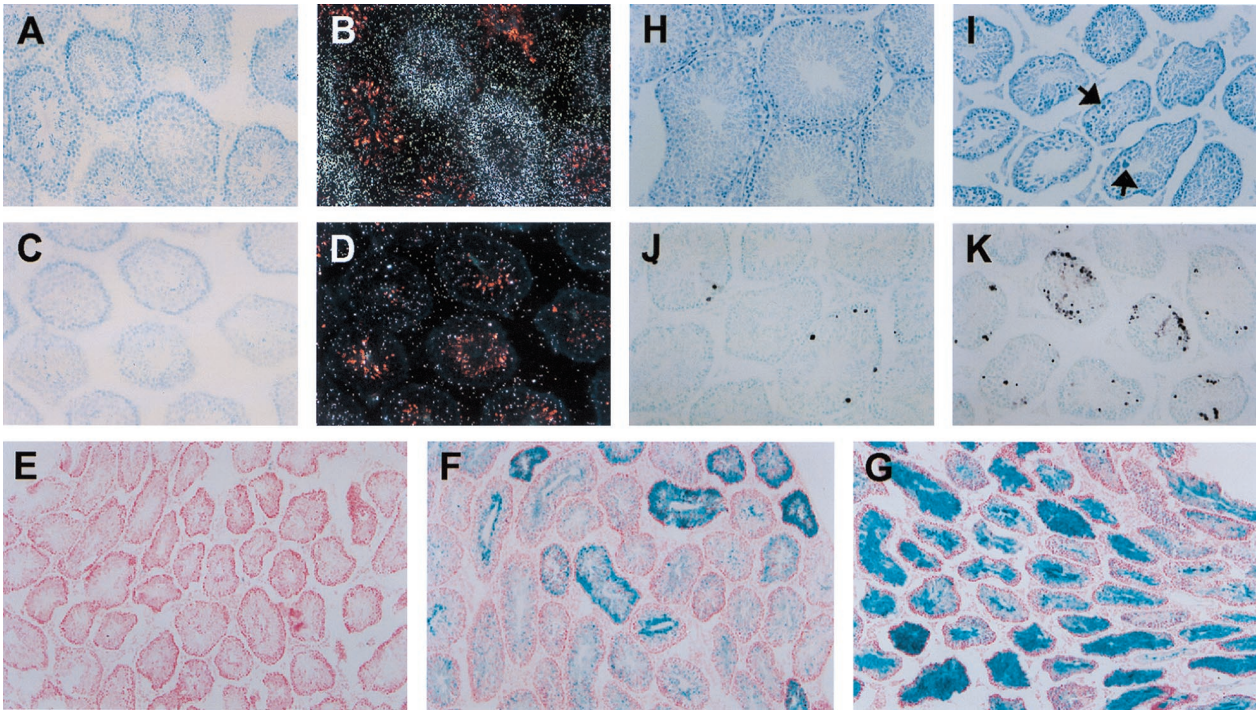


FIG. 4. Deficient INK4d expression and apoptosis in testis. (Panels A to D) In situ hybridization, using an *INK4d* antisense riboprobe, was performed on testis sections from 6-week-old wild-type (A and B) and *INK4d*-deficient (C and D) mice. Panel A shows a toluidine blue-stained bright field of panel B, and panel C shows a bright field of panel D, all at equal magnification. (Panels E to G) Because the β-*geo* cassette is encoded by the disrupted *INK4d* gene, tissues containing the mutant allele express β-galactosidase, which was detected in tissues from hemizygous (F) and *INK4d*-null mice (G). Wild-type mice that lack the β-*geo* cassette exhibit only background staining (E). All tissues were counterstained with neutral red dye. *INK4d* expression is heterogeneous throughout the tubules and is reduced by about 50% in heterozygous animals (cf. Fig. 2B). Under matched staining conditions, more intense and more uniform staining for β-galactosidase is therefore observed in tubules from *INK4d*-deficient mice (G) than in testes from hemizygous animals (F). (Panels H to K) Sections from testes of wild-type (panels H and J) and *INK4d*-deficient mice (panels I and K) were photographed and reproduced at equal magnification and were stained with toluidine blue (H and I) or subjected to TUNEL assay (J and K). Increased apoptosis in *INK4d*-deficient animals correlated with testicular atrophy.

In general, the highest levels of $p19^{INK4d}$ protein expression occur in testis, spleen, thymus, and brain (54). Although *INK4d* loss partially compromised germ cell development in male mice, their sperm counts remained at sufficient levels to maintain their fertility, thereby producing no overt consequences. We saw no abnormalities in lymphoid T- or B-cell development, differentiation, or response to lymphokines, nor did we detect defects in the proliferation rate, cell cycle distribution, or mitogenic response of cultured MEFs or bone marrow-derived macrophages. The latter data are concordant with surveys from our own institution that failed to implicate genetic alterations of *INK4d* in pediatric hematologic malignancies involving myeloid or lymphoid cells (D. Reardon, J. Downing, C. J. Sherr, and M. F. Roussel, unpublished data).

The one place that *INK4d* expression has been relatively well characterized is in the central nervous system (55). *INK4d* is expressed during development of the brain from embryonic day 11.5 onward, primarily in postmitotic neurons. During development of the neocortex, asymmetric divisions give rise to differentiated neurons that exit the cell cycle and migrate to their final position in the brain (4, 6, 48), and it is only these postmitotic cells that express $p19^{INK4d}$ (55). *INK4d* expression is maintained into adulthood not only in postmitotic neurons of the cerebral cortex, but in neurons of the dentate gyrus, the pyramidal layer of the hippocampus, and in regions of the cerebellum, thalamus, and brainstem. Cyclin D1 levels also remain elevated in postmitotic neurons (10, 20), so that the persistence of $p19^{INK4d}$ might prevent reactivation of CDK4 and CDK6 in this context. This raised the possibility that *INK4d* loss might affect neuronal development or lead to brain tumors. Moreover, down regulation of $p19^{INK4d}$ in the dentate gyrus after kainic acid-induced seizures previously indicated that excitotoxic stress could modify *INK4d* expression in nondividing cells (55). Together, these data alluded to possible roles for *INK4d* in maintaining neurons in a quiescent state and/or modifying apoptotic responses to stress-induced signals, predictions that, at face value, were negated by the results reported here. The absence of brain tumors in the *INK4d*-deficient mouse after more than 2 years of follow up is consistent with our surveys of pediatric brain tumors, including medulloblastoma, ependymoma, and both low- and high-grade gliomas, in which we also failed to document any *INK4d* alterations (D. Reardon, J. Downing, C. J. Sherr, and M. F. Roussel, unpublished data).

*INK4c* is another *INK4* family member expressed in the developing brain, but it resides exclusively in neuronal progenitors (55). Its inactivation also failed to cause neurologic defects, whether disrupted alone or in conjunction with the *INK4d* gene (M. Barbacid, F. Zindy, C. J. Sherr, and M. F. Roussel, unpublished data). On the other hand, analysis of expression of other CKIs revealed that *INK4d* and *Kip1* were coexpressed in similar regions of the brain, particularly in the cerebral cortex (22, 55). In support of the idea that these two CKIs might play compensating roles in neocortical development, recent data from our laboratory indicate that codeletion of *INK4d* and *Kip1* leads to ectopic neuronal proliferation in neonatal animals (53a).

Results of this type point to the need for generating mice that lack more than one CKI, in order to explore their potential for functional compensation in different tissues. There are

already several precedents. Mice lacking *Kip1* develop organomegaly and middle lobe pituitary hyperplasia (8, 19, 28), while those lacking *INK4c* develop middle lobe pituitary tumors late in life (9). However, animals that have lost both genes develop aggressive middle lobe pituitary tumors with a much earlier onset, suggesting that *INK4c* and *Kip1* play overlapping roles in controlling pituitary development (9). Presumably, these results reflect modulation of Rb function, since $Rb^{+/-}$ animals also develop middle lobe pituitary tumors with accompanying loss of the wild-type *Rb* allele (13, 14). Cooperativity in regulating the cell cycle and controlling differentiation of the lens and placenta has been similarly documented in mice deleted for *Kip1* and *Kip2* (52), whereas muscle development is severely compromised in mice lacking *Cip1* and *Kip2*, but not either gene alone (53).

***INK4d*-deficient mice display testicular atrophy associated with increased apoptosis.** The single most remarkable finding in *INK4d*-deficient mice was marked testicular atrophy associated with increased apoptosis in germ cells, a site where $p19^{INK4d}$ is normally expressed (reference 54 and this work). Spermatogenesis provides a unique in vivo model for studying cell cycle exit and differentiation. Spermatogonia undergo mitosis, whereas spermatocytes undergo meiosis, yielding spermatids that differentiate into mature spermatozoa. *CDK4* is expressed in spermatogonia and in early stage primary spermatocytes but does not contribute to later stages of germ cell development (18, 38). Patterns of *INK4d* expression imply that $p19^{INK4d}$ can be found in germ cells undergoing meiosis and during differentiation from spermatids to spermatozoa, so $p19^{INK4d}$ may help to prepare cells for meiosis by downregulating CDK4. Conversely, the marked increase in apoptosis in germ cells lacking *INK4d* suggests that cells that do not properly exit the mitotic cycle can be subsequently eliminated through activation of checkpoint controls that are triggered when S-phase entry occurs inappropriately. There are many cell systems in which apoptotic events depend upon proper Rb function (15, 49), consistent with the notion that $p19^{INK4d}$ exerts its known effects through the Rb pathway.

Spermatogenesis is only partially compromised in *INK4d*-deficient animals, again suggesting that other CKIs might also be involved in that process. We indeed found by in situ hybridization that *INK4c* was coexpressed with *INK4d* during spermatogenesis (data not shown), raising the possibility that *INK4c* might partially compensate for the lack of *INK4d*. Preliminary results from crosses between *INK4d*- and *INK4c*-deficient mice have revealed male sterility with virtual absence of spermatozoa in the lumina of seminiferous tubules. This indicates that *INK4c* and *INK4d* cooperate in male germ cell development and are both required for the production of mature spermatozoa. (F. Zindy, P. den Besten, P. Cohen, M. Barbacid, C. J. Sherr, and M. F. Roussel, unpublished data). Intriguingly, "knock-in" animals expressing a CDK4 mutant (R24C) that is resistant to INK4 inhibition show Leydig cell hyperplasia later in life (34), effects that we have also begun to observe in aging *INK4c-INK4d* double-null animals. To our knowledge, effects on male fertility represent the first pending example of functional cooperation between different *INK4* family members during development.

## ACKNOWLEDGMENTS

We thank Paula Cohen (Albert Einstein University, New York, N.Y.) for help in the identification of testicular cells, Sandra d'Azzo for suggestions in initiating this project, members of the Roussel and Sherr laboratory for helpful discussions, Esther Latres and Maria Barbacid for communicating unpublished results, and John Cleveland for critical review of the manuscript. We also thank Anne-Marie Hamilton and Suzette Wingo for the characterization of B and T cells and Joseph Watson and Manjula Paruchuri for excellent technical assistance. We are indebted to Catherine Poquette, Xialong Luo, and James Boyette from the Department of Biostatistics at St. Jude Children's Research Hospital for statistical analysis.

This work was supported in part by NIH grant PO1 CA-71907, Cancer Core Grant CA-21765, and the American Lebanese Syrian Associated Charities of St. Jude Children's Research Hospital. C.J.S. is an investigator of the Howard Hughes Medical Institute.

## REFERENCES

1. **Alevizopoulos, K., J. Vlach, S. Hennecke, and B. Amati.** 1997. Cyclin E and c-Myc promote cell proliferation in the presence of $p16^{INK4a}$ and of hypophosphorylated retinoblastoma family proteins. EMBO J. **16:**5322–5333.
2. **Blain, S. W., E. Montalvo, and J. Massague.** 1997. Differential interaction of the cyclin-dependent kinase (Cdk) inhibitor $p27^{Kip1}$ with cyclin A-Cdk2 and cyclin D2-Cdk4. J. Biol. Chem. **272:**25863–25872.
3. **Brotherton, D. H., V. Dhanaraj, S. Wick, L. Brizuela, P. J. Domaille, E. Volyanik, X. Xu, E. Parisini, B. O. Smith, S. J. Archer, M. Serrano, S. L. Brenner, T. L. Blundell, and E. D. Laue.** 1998. Crystal structure of the complex of the cyclin D-dependent kinase Cdk6 bound to the cell-cycle inhibitor $p19^{INK4d}$. Nature **395:**244–250.
4. **Caviness, V. S., Jr., T. Takahashi, and R. S. Nowakowski.** 1995. Numbers, time and neocortical neuronogenesis: a general developmental and evolutionary model. Trends Neurosci. **18:**379–383.
5. **Cheng, M., P. Olivier, J. A. Diehl, M. Fero, M. F. Roussel, J. M. Roberts, and C. J. Sherr.** 1999. The $p21^{Cip1}$ and $p27^{Kip1}$ CDK "inhibitors" are essential activators of cyclin D-dependent kinases in murine fibroblasts. EMBO J. **18:** 1571–1583.
6. **Chenn, A., and S. K. McConnell.** 1995. Cleavage orientation and the asymmetric inheritance of Notch1 immunoreactivity in mammalian neurogenesis. Cell **82:**631–642.
7. **Dyson, N.** 1998. The regulation of E2F by pRB-family proteins. Genes Dev. **12:**2245–2262.
8. **Fero, M. L., M. Rivkin, M. Tasch, P. Porter, C. E. Carow, E. Firpo, K. Polyak, L.-H. Tsai, V. Broudy, R. M. Perlmutter, K. Kaushansky, and J. M. Roberts.** 1996. A syndrome of multiorgan hyperplasia with features of gigantism, tumorigenesis, and female sterility in $p27^{Kip1}$-deficient mice. Cell **85:**733–744.
9. **Franklin, D. S., V. L. Godfrey, H. Lee, G. I. Kovalev, R. Schoonhoven, S. Chen-Kiang, L. Su, and Y. Xiong.** 1998. CDK inhibitors $p18^{INK4c}$ and $p27^{Kip1}$ mediate two separate pathways to collaboratively suppress pituitary tumorigenesis. Genes Dev. **12:**2899–2911.
10. **Freeman, R. S., and E. M. Johnson, Jr.** 1994. Analysis of cell cycle-related gene expression in postmitotic neurons: selective induction of cyclin D1 during programmed cell death. Neuron **12:**343–355.
11. **Hannon, G. J., and D. Beach.** 1994. $p15^{INK4B}$ is a potential effector of TGFβ-induced cell cycle arrest. Nature **371:**257–261.
12. **Hirai, H., M. F. Roussel, J. Kato, R. A. Ashmun, and C. J. Sherr.** 1995. Novel INK4 proteins, p19 and p18, are specific inhibitors of the cyclin D-dependent kinases CDK4 and CDK6. Mol. Cell. Biol. **15:**2672–2681.
13. **Hu, N., A. Gutsmann, D. C. Herbert, A. Bradley, W.-H. Lee, and E. Y.-H. P. Lee.** 1994. Heterozygous *Rb*-$1^{D20/+}$ mice are predisposed to tumors of the pituitary gland with a nearly complete penetrance. Oncogene **9:**1021–1027.
14. **Jacks, T., A. Fazeli, E. M. Schmitt, R. T. Bronson, M. A. Goodell, and R. A. Weinberg.** 1992. Effects of an Rb mutation in the mouse. Nature **359:**295–300.
15. **Jacks, T., and R. A. Weinberg.** 1996. Cell-cycle control and its watchman. Nature **381:**643–644.
16. **Jiang, H., H. S. Chou, and L. Zhu.** 1998. Requirement of cyclin E-cdk2 inhibition in $p16^{INK4a}$-mediated growth suppression. Mol. Cell. Biol. **18:** 5284–5290.
17. **Kamijo, T., F. Zindy, M. F. Roussel, D. E. Quelle, J. R. Downing, R. A. Ashmun, G. Grosveld, and C. J. Sherr.** 1997. Tumor suppression at the mouse *INK4a* locus mediated by the alternative reading frame product $p19^{ARF}$. Cell **91:**649–659.
18. **Kang, M. J., M. K. Kim, A. Terhune, J. K. Park, Y. H. Kim, and G. Y. Koh.** 1997. Cytoplasmic localization of cyclin D3 in seminiferous tubules during testicular development. Exp. Cell Res. **234:**27–36.
19. **Kiyokawa, H., R. D. Kineman, K. O. Manova-Todorova, V. C. Soares, E. S. Hoffman, M. Ono, D. Khanam, A. C. Hayday, L. A. Frohman, and A. Koff.** 1996. Enhanced growth of mice lacking the cyclin-dependent kinase inhibitor function of $p27^{Kip1}$. Cell **85:**721–732.
20. **Kranenburg, O., A. J. van der Eb, and A. Zantema.** 1996. Cyclin D1 is an essential mediator of apoptotic neuronal cell death. EMBO J. **15:**46–54.
21. **LaBaer, J., M. D. Garrett, L. F. Stevenson, J. M. Slingerland, C. Sandhu, H. S. Chou, A. Fattaey, and E. Harlow.** 1997. New functional activities for the p21 family of CDK inhibitors. Genes Dev. **11:**847–862.
22. **Lee, M.-H., M. Nikolic, C. A. Bapista, E. Lai, L.-H. Tsai, and J. Massagué.** 1996. The brain-specific activator p35 allows Cdk5 to escape inhibition by $p27^{Kip1}$ in neurons. Proc. Natl. Acad. Sci. USA **93:**3259–3263.

23. **Lukas, J., T. Herzinger, K. Hansen, M. C. Moroni, D. Resnitzky, K. Helin, S. I. Reed, and J. Bartek.** 1997. Cyclin E-induced S phase without activation of the Rb/E2F pathway. Genes Dev. **11:**1479–1492.
24. **McConnell, B. B., F. J. Gregory, F. J. Stott, E. Hara, and G. Peters.** 1999. Induced expression of $p16^{INK4a}$ inhibits both CDK4- and CDK2-associated kinase activity by reassortment of cyclin-CDK-inhibitor complexes. Mol. Cell. Biol. **19:**1981–1989.
25. **Mitra, J., C. Y. Dai, K. Somasundaram, W. El-Deiry, K. Satamoorthy, M. Herlyn, and G. H. Enders.** 1999. Induction of $p21^{WAF1/Cip1}$ and inhibition of Cdk2 mediated by the tumor suppressor $p16^{INK4a}$. Mol. Cell. Biol. **19:**3916–3928.
26. **Morse, L., D. Chen, D. Franklin, Y. Xiong, and S. Chen-Kiang.** 1997. Induction of cell cycle arrest and B cell terminal differentiation by CDK inhibitor p18 (INK4c) and IL-6. Immunity **6:**47–56.
27. **Naito, M., and J. DiGiovanni.** 1989. Genetic background and development of skin tumors, p. 187–212. *In* C. J. Conti, T. J. Slaga, and A. J. P. Klein-Szanto (ed.), Carcinogenesis, vol. III. Skin tumors: experimental and clinical aspects. Raven Press, New York, N.Y.
28. **Nakayama, K., N. Ishida, M. Shirane, A. Inomata, T. Inoue, N. Shishido, I. Horii, and D. Y. Loh.** 1996. Mice lacking $p27^{Kip1}$ display increased body size, multiple organ hyperplasia, retinal dysplasia, and pituitary tumors. Cell **85:** 707–720.
29. **Oberdick, J., J. D. Wallace, A. Lewin, and R. J. Smeyne.** 1994. Transgenic expression to monitor dynamic organization of neuronal development: use of *Escherichia coli LacZ* gene product, β-galactosidase. Methods Neurosci. **5:** 54–62.
30. **O'Farrell, A.-M., D. A. Parry, F. Zindy, M. F. Roussel, E. Lees, K. W. Moore, and A. L.-F. Mui.** Inhibition of proliferation by IL-10 is mediated by Stat3-dependent induction of $p19^{INK4d}$. J. Immunol., in press.
31. **Parry, D. A., D. Mahony, K. Wills, and E. Lees.** 1999. Cyclin D-CDK subunit arrangement is dependent on the availability of competing INK4 and p21 class inhibitors. Mol. Cell. Biol. **19:**1775–1783.
32. **Pavletich, N. P.** 1999. Mechanisms of cyclin-dependent kinase regulation: structures of Cdks, their cyclin activators, and Cip and INK4 inhibitors. J. Mol. Biol. **287:**821–828.
33. **Quelle, D. E., F. Zindy, R. A. Ashmun, and C. J. Sherr.** 1995. Alternative reading frames of the INK4a tumor suppressor gene encode two unrelated proteins capable of inducing cell cycle arrest. Cell **83:**993–1000.
34. **Rane, S. G., P. Dubus, R. V. Mettus, E. J. Galbreath, G. Boden, E. P. Reddy, and M. Barbacid.** 1999. Loss of Cdk4 expression causes insulin-deficient diabetes and Cdk4 activation results in β-islet cell hyperplasia. Nat. Genet. **22:**44–52.
35. **Reiners, J. J., Jr., S. Nesnow, and T. J. Slaga.** 1984. Murine susceptibility to two-stage skin carcinogenesis is influenced by the agent used for promotion. Carcinogenesis **5:**301–307.
36. **Reynisdóttir, I., and J. Massagué.** 1997. The subcellular locations of $p15^{INK4b}$ and $p27^{Kip1}$ coordinate their inhibitory interactions with cdk4 and cdk2. Genes Dev. **11:**492–503.
37. **Reynisdóttir, I., K. Polyak, A. Iavarone, and J. Massagué.** 1995. Kip/Cip and Ink4 cdk inhibitors cooperate to induce cell cycle arrest in response to TGF-β. Genes Dev. **9:**1831–1845.
38. **Rhee, K., and D. J. Wolgemuth.** 1995. Cdk family genes are expressed not only in dividing but also in terminally differentiated mouse germ cells, suggesting their possible function during both cell division and differentiation. Dev. Dyn. **204:**406–420.
39. **Roberts, J. M.** 1999. Evolving ideas about cyclins. Cell **98:**129–132.

39a. **Roussel, M. F.** 1999. The INK4 family of cell cycle inhibitors in cancer. Oncogene **18:**5311–5317.

40. **Ruas, M., and G. Peters.** 1998. The $p16^{INK4a}$/CDKN2A tumor suppressor and its relatives. BBA Rev. Cancer **1378:**F115–F177.
41. **Russo, A. A., L. Tong, J.-O. Lee, P. D. Jeffrey, and N. P. Pavletich.** 1998. Structural basis for inhibition of the cyclin-dependent kinase Cdk6 by the tumour suppressor $p16^{INK4a}$. Nature **395:**237–243.
42. **Serrano, M., G. J. Hannon, and D. Beach.** 1993. A new regulatory motif in cell cycle control causing specific inhibition of cyclin D/CDK4. Nature **366:** 704–707.
43. **Serrano, M., H.-W. Lee, L. Chin, C. Cordon-Cardo, D. Beach, and R. A. DePinho.** 1996. Role of the INK4a locus in tumor suppression and cell mortality. Cell **85:**27–37.
44. **Sherr, C., and J. M. Roberts.** 1999. Positive and negative regulation by CDK inhibitors. Genes Dev. **13:**1501–1512.
45. **Sherr, C. J.** 1993. Mammalian $G_1$ cyclins. Cell **73:**1059–1065.
46. **Sherr, C. J., and J. M. Roberts.** 1995. Inhibitors of mammalian G1 cyclin-dependent kinases. Genes Dev. **9:**1149–1163.
47. **Soos, T. J., H. Kiyokawa, J. S. Yan, M. S. Rubin, A. Giordano, A. DeBlasio, S. Bottega, B. Wong, J. Mendelsohn, and A. Koff.** 1996. Formation of p27-CDK complexes during the human mitotic cell cycle. Cell Growth Differ. **7:** 135–146.
48. **Takahashi, T., R. S. Nowakowshi, and V. S. Caviness.** 1995. The cell cycle of the pseudostratified venticular epithelium of the embryonic murine cerebral wall. J. Neurosci. **15:**6046–6057.
49. **Weinberg, R. A.** 1995. The retinoblastoma protein and cell cycle control. Cell **81:**323–330.
50. **Whitlock, C. A., and O. N. Witte.** 1987. Long-term culture of murine bone marrow precursors of B lymphocytes. Methods Enzymol. **150:**275–286.
51. **Zhang, H., G. J. Hannon, and D. Beach.** 1994. p21-containing cyclin kinases exist in both active and inactive states. Genes Dev. **8:**1750–1758.
52. **Zhang, P., C. Wong, R. DePinho, J. W. Harper, and S. J. Elledge.** 1998. Cooperation between the *Cdk* inhibitors $p27^{KIP1}$ and $p57^{KIP2}$ in the control of tissue growth and development. Genes Dev. **12:**3162–3167.
53. **Zhang, P., C. Wong, D. Liu, M. Finegold, J. W. Harper, and S. J. Elledge.** 1999. $p21^{Cip1}$ and $p57^{Kip2}$ control muscle differentiation at the myogenin step. Genes Dev. **13:**213–224.

53a. **Zindy, F., J. J. Cunningham, C. J. Sherr, S. Jogal, R. J. Smeyne, and M. F. Roussel.** Postnatal neuronal proliferation in mice lacking INK4a and KIP1 inhibitors of cyclin-dependent kinases. Proc. Natl. Acad. Sci. USA, in press.

54. **Zindy, F., D. E. Quelle, M. F. Roussel, and C. J. Sherr.** 1997. Expression of the $p16^{INK4a}$ tumor suppressor versus other INK4 family members during mouse development and aging. Oncogene **15:**203–211.
55. **Zindy, F., H. Soares, K.-H. Herzog, J. Morgan, C. J. Sherr, and M. F. Roussel.** 1997. Expression of INK4 inhibitors in cyclin D-dependent kinases during mouse brain development. Cell Growth Differ. **8:**1139–1150.